Supplementary Information

Changing patterns of global nitrogen deposition driven by socio-economic development

Jianxing Zhu[1,#], Yanlong Jia[2,#], Guirui Yu[1,3,*], Qiufeng Wang[1,3], Nianpeng He[4], Zhi Chen[1,3], Honglin He[1,3], Xianjin Zhu[5], Pan Li[6], Fusuo Zhang[7], Xuejun Liu[7], Keith Goulding[8], David Fowler[9] and Peter Vitousek[10]

1 Key Laboratory of Ecosystem Network Observation and Modeling, Institute of Geographic Sciences and Natural Resources Research, Chinese Academy of Sciences, Beijing, China.

2 College of Forestry, Hebei Agricultural University, Baoding, China.

3 College of Resources and Environment, University of Chinese Academy of Sciences, Beijing, China.

4 Key Laboratory of Sustainable Forest Ecosystem Management-Ministry of Education, Northeast Forestry University, Harbin, China.

5 College of Agronomy, Shenyang Agricultural University, Shenyang, China.

6 Institute of Surface-Earth System Science, School of Earth System Science, Tianjin University, Tianjin, China.

7 State Key Laboratory of Nutrient Use and Management, College of Resources and Environmental Sciences, National Academy of Agriculture Green Development, China Agricultural University, Beijing, China.

8 Sustainable Agricultural Sciences Department, Rothamsted Research, Harpenden, UK.

9 Centre for Ecology and Hydrology, Penicuik, UK.

10 Department of Biology, Stanford University, Stanford, USA.

# These authors contributed equally: Jianxing Zhu and Yanlong Jia.

* Correspondence author: Guirui Yu (yugr@igsnrr.ac.cn)

This file includes:

Supplementary Figure 1-17

Supplementary Table 1-8

Supplementary References

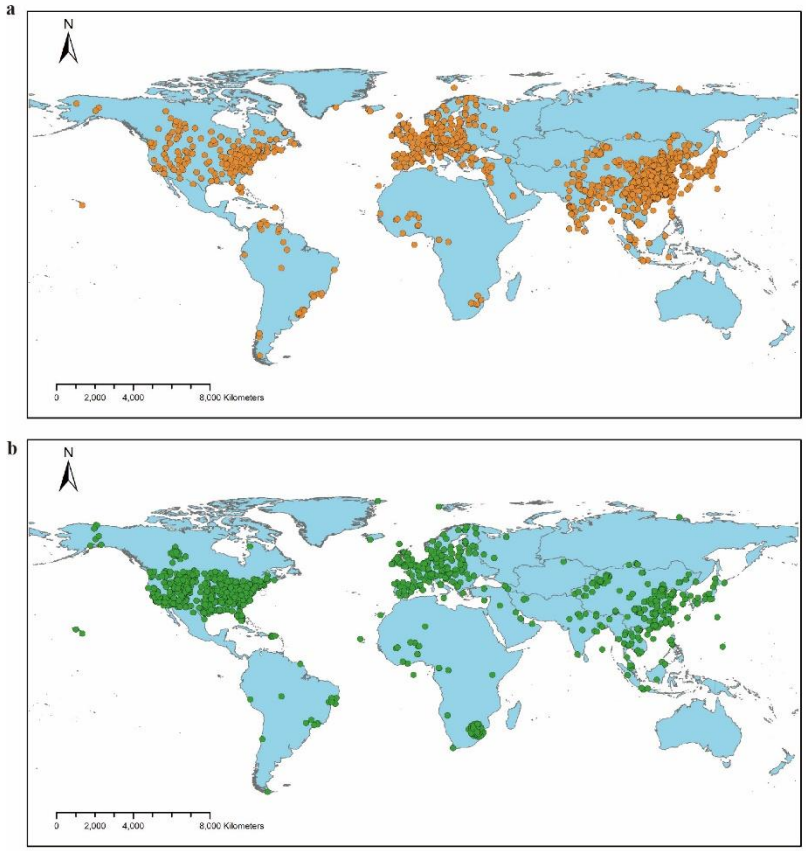

Supplementary Figure 1 | Monitoring sites for nitrogen deposition. (a) Spatial distribution of wet deposition observation sites (orange dots); (b) Spatial distribution of dry deposition observation sites (green dots). These sites are sourced from the Chinese Wet Deposition Observation Network (ChinaWD), the Co-operative Programme for Monitoring and Evaluation of the Long-Range Transmission of Air Pollutants in Europe (European Monitoring and Evaluation Programme, EMEP), the Clean Air Status and Trends Network (CASTNET), the Air Quality System (AQS), and the Ammonia Monitoring Network (AMoN) in the United States, the Canadian Air and Precipitation Monitoring Network (CAPMoN) and the National Air Pollution Surveillance Program (NAPS) in Canada, the Acid Deposition Monitoring Network in East Asia (EANET), the International Network to Study Deposition and Atmospheric Composition in Africa (INDAAF), the Nationwide Nitrogen Deposition Monitoring Network (NNDMN) from China Agricultural University, and 1,390 published papers.

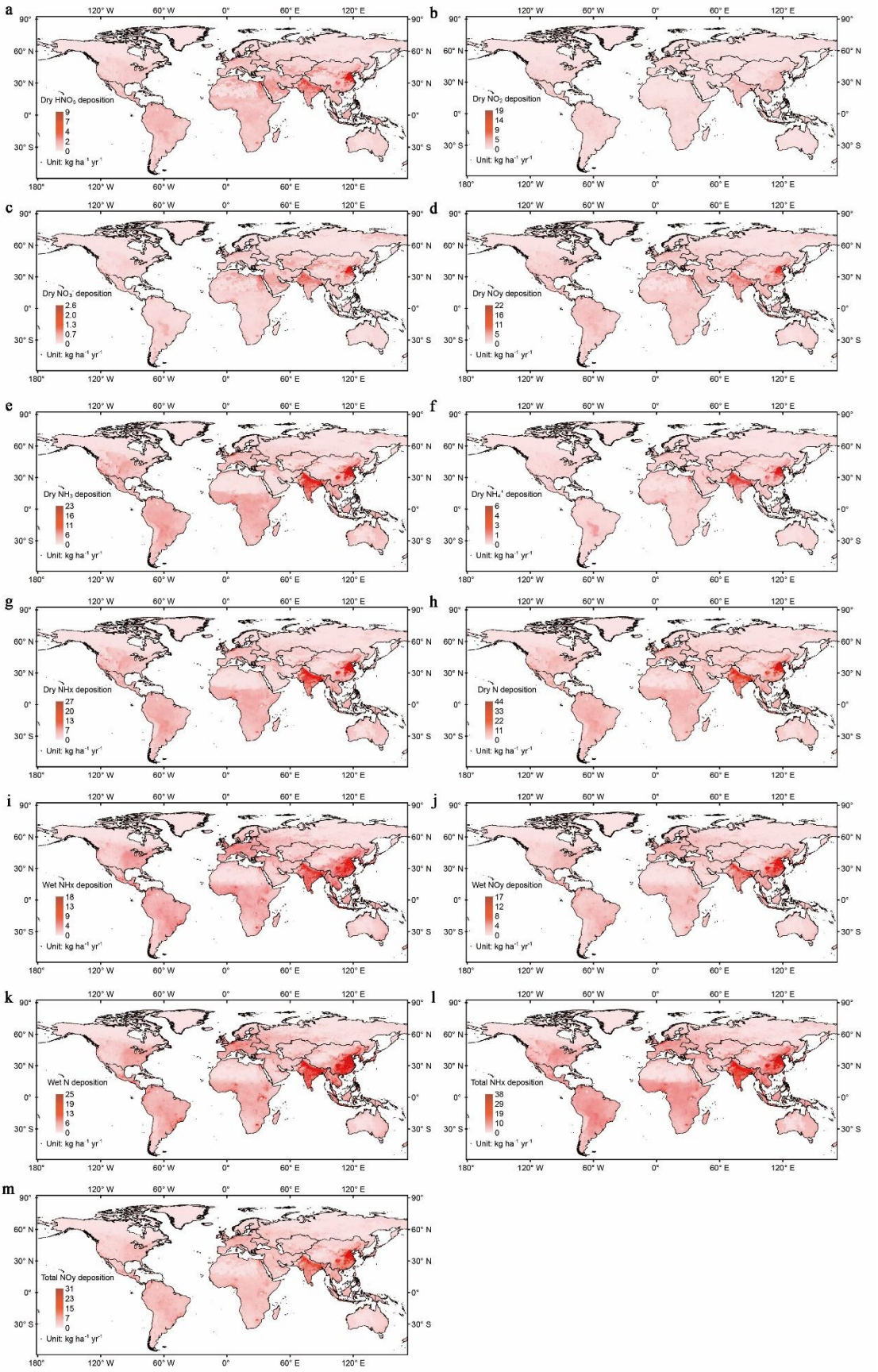

Supplementary Figure 2 | Spatial maps of global nitrogen deposition in 2020. (a) Spatial distribution of dry

HNO_3 deposition in 2020. (b) Spatial distribution of dry NO_2 deposition in 2020. (c) Spatial distribution of dry NO_3^- deposition in 2020. (d) Spatial distribution of dry NO_y deposition in 2020. (e) Spatial distribution of dry NH_3 deposition in 2020. (f) Spatial distribution of dry NH_4^+ deposition in 2020. (g) Spatial distribution of dry NH_x deposition in 2020. (h) Spatial distribution of dry nitrogen (N) deposition in 2020. (i) Spatial distribution of wet NH_x deposition in 2020. (j) Spatial distribution of wet NO_y deposition in 2020. (k) Spatial distribution of wet N deposition in 2020. (l) Spatial distribution of total NH_x deposition in 2020. (m) Spatial distribution of total NO_y deposition in 2020. The results represent the average values from three random forest models. Data for Antarctica are not included.

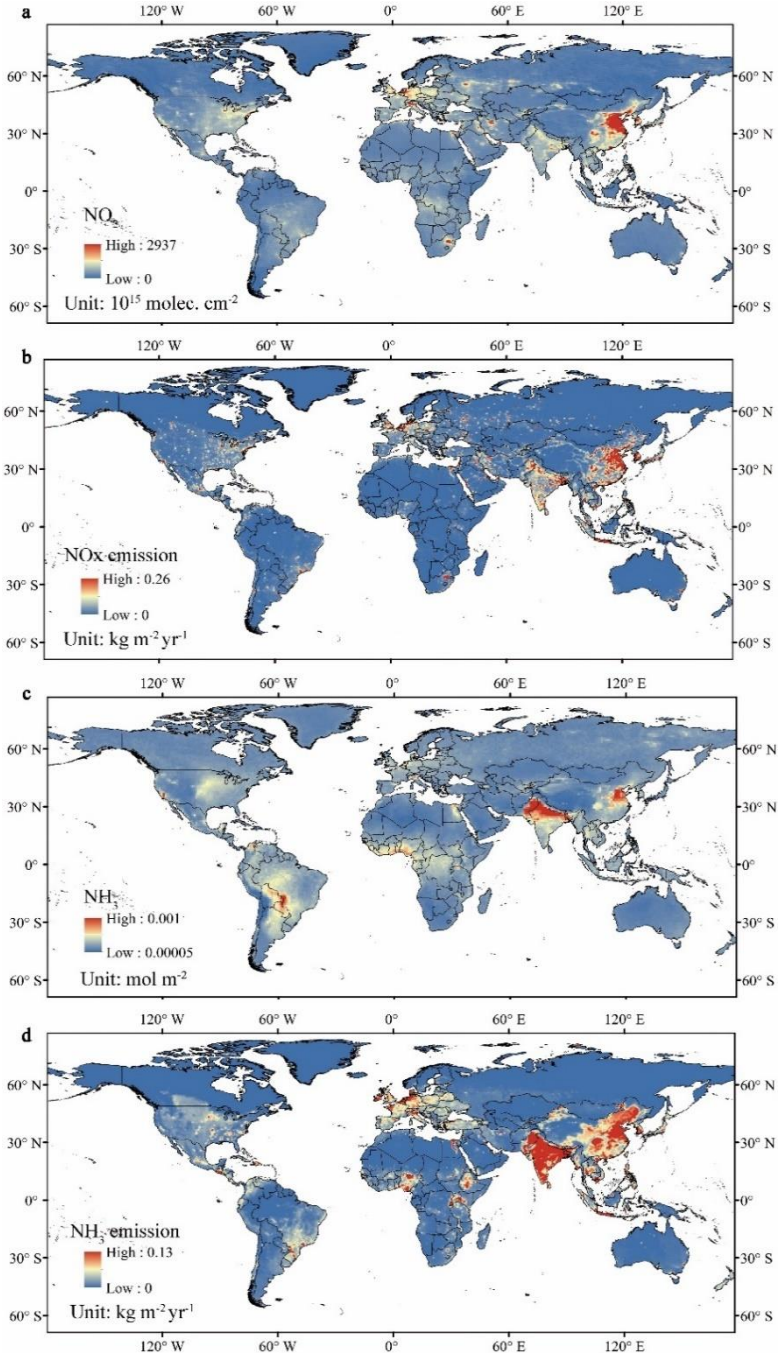

Supplementary Figure 3 | The spatial patterns of satellite nitrogen column concentrations and reactive nitrogen emissions in 2020. (a) NO_2 column concentration in 2020 from the Ozone Monitoring Instrument (OMI). (b) NOx emission in 2020 from the Community Emission Data System (CEDS) emission inventory. (c) NH_3 column concentration in 2020 from the Infrared Atmospheric Sounding Interferometer (IASI). (d) NH_3 emission in 2020 from the CEDS emission inventory. Data for the Antarctic are not included.

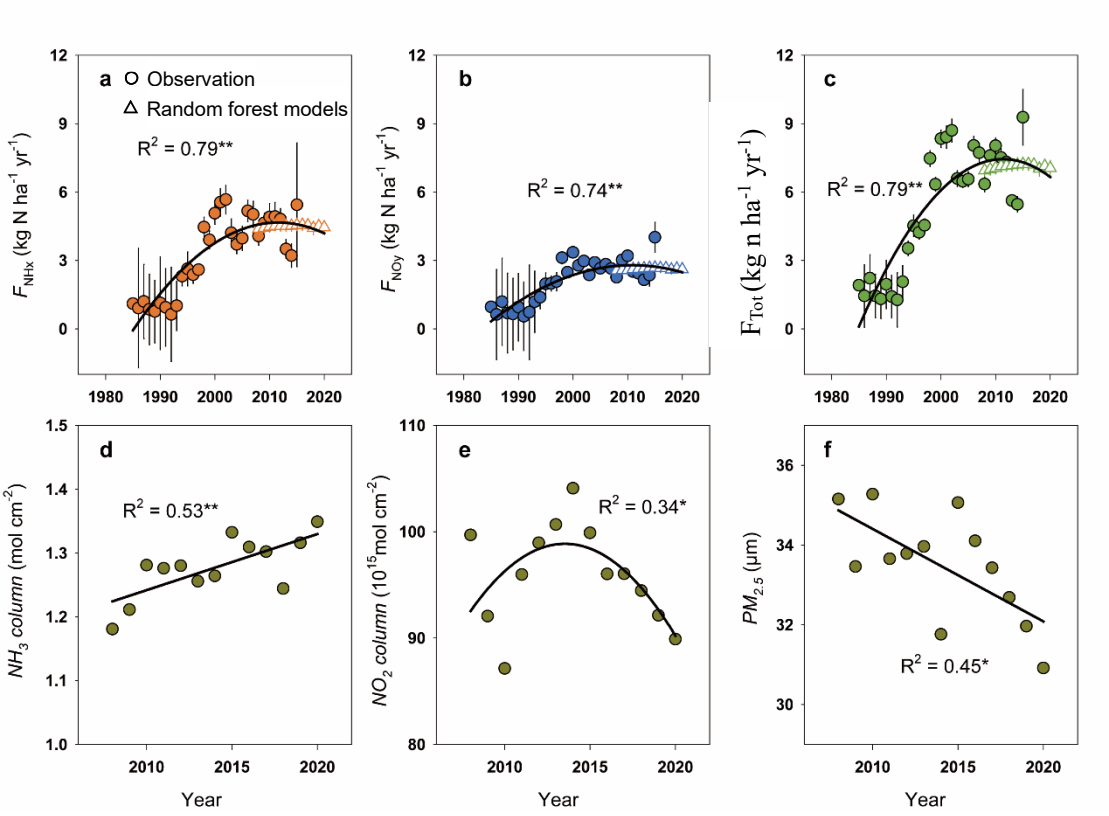

Supplementary Figure 4 | Temporal dynamics of nitrogen deposition, satellite NH_3 and NO_2 column concentrations, and $PM_{2.5}$ in Africa. (a) Temporal dynamics of NHx deposition (F_{NHx}) in Africa. (b) Temporal dynamics of NOy deposition (F_{NOy}) in Africa. (c) Temporal dynamics of total nitrogen deposition (F_{Tot}) in Africa. (d) Temporal dynamics of NH_3 column concentration in Africa from the Infrared Atmospheric Sounding Interferometer (IASI). (e) Temporal dynamics of NO_2 column concentration in Africa from the Ozone Monitoring Instrument (OMI). (f) Temporal dynamics of $PM_{2.5}$ in Africa. For (a–c), circles represent direct observations with error bars showing SE (variation among monitoring sites), and triangles represent estimates from random forest models with error bars showing SE (variation among the three models' results). R^2 is the coefficient of determination. ** and * represent significance levels at P = 0.01 and P = 0.05, respectively.

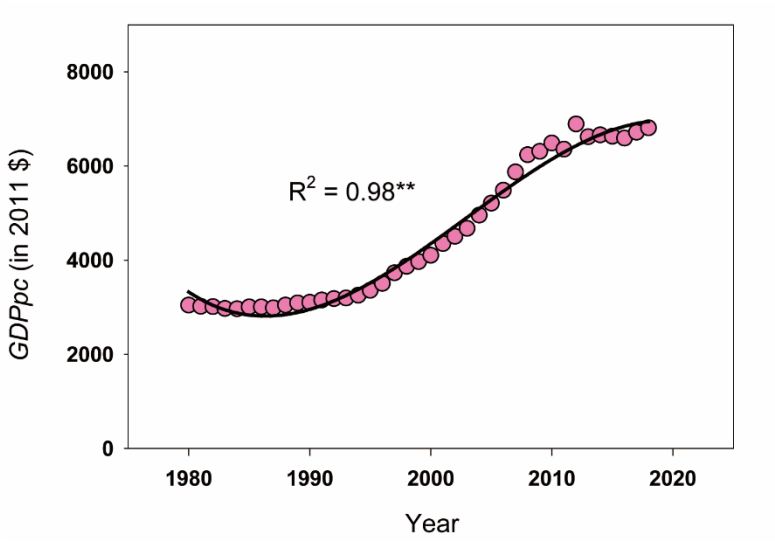

Supplementary Figure 5 | Temporal dynamics of gross domestic product per capita in Africa. Gross domestic product per capita (GDPpc) data is obtained from the Maddison Project Database 2020. R^2 represents the coefficient of determination. ** and * indicate significance levels at P = 0.01 and P = 0.05, respectively.

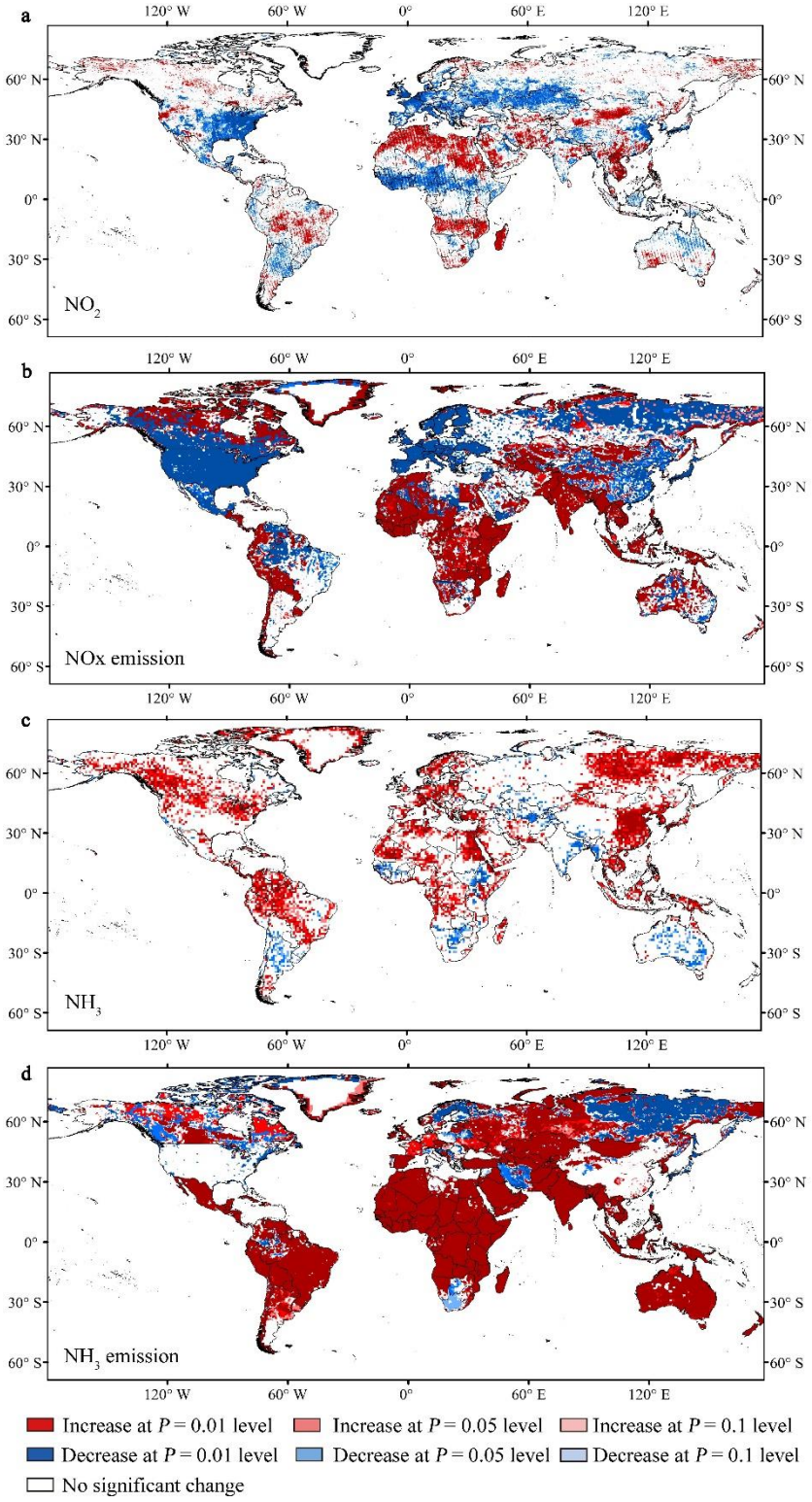

Supplementary Figure 6 | Trends in satellite nitrogen column concentrations and reactive nitrogen emissions from 2008 to 2020. (a) Trend analysis of satellite NO_2 column concentration from the Ozone Monitoring Instrument (OMI) during 2008–2020. (b) Trend analysis of NOx emission from the Community Emission Data System (CEDS) emission inventory during 2008–2020. (c) Trend analysis of satellite NH_3 column concentration from the Infrared

Atmospheric Sounding Interferometer (IASI) during 2008–2020. (d) Trend analysis of NH_3 emission from the CEDS emission inventory during 2008–2020. The Mann–Kendall nonparametric test was used to assess the significance of these trends. Data for Antarctica are not included.

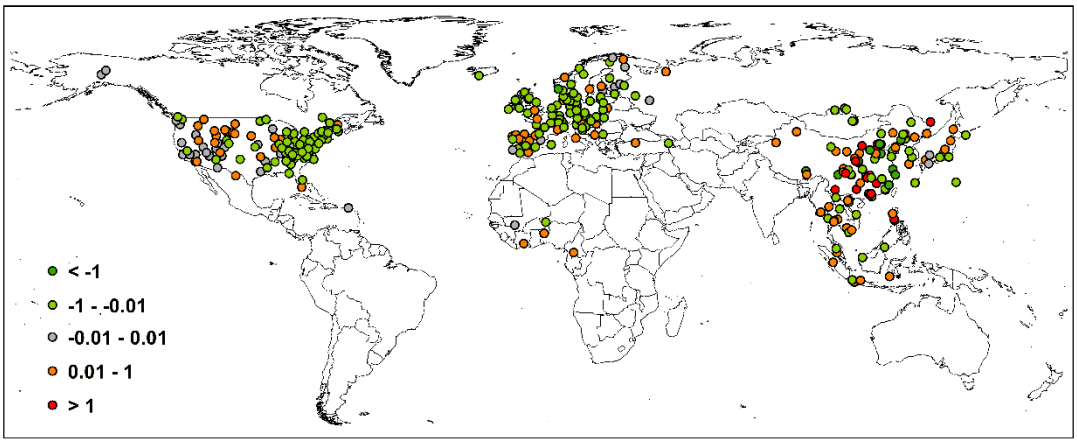

Supplementary Figure 7 | Trends in wet nitrogen deposition at long-term monitoring sites (kg N ha^{-1} yr^{-1}). The dots represent the trends in wet deposition at sites with five years of continuous monitoring since 2000. Green dots indicate decreases and red dots indicate increases. Data for the Antarctic are not included.

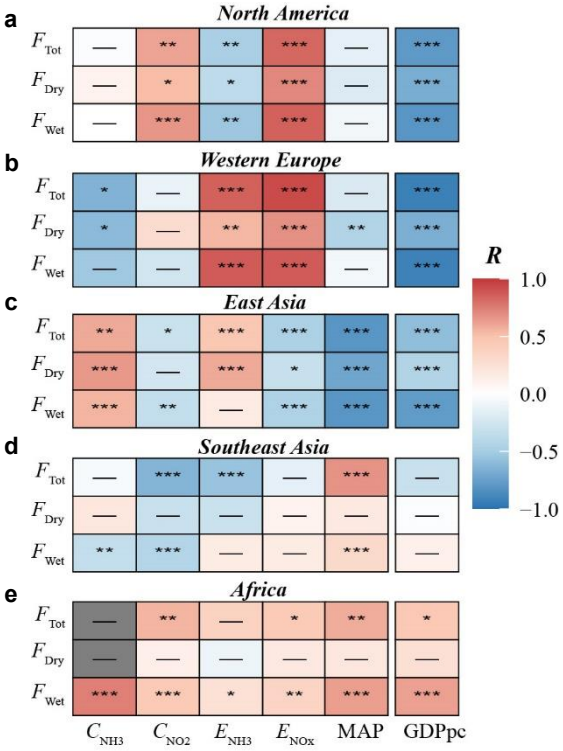

Supplementary Figure 8 | Heat map of nitrogen deposition and its influencing factors. (a) Correlations in North America. (b) Correlations in Western Europe. (c) Correlations in East Asia. (d) Correlations in Southeast Asia. (e) Correlations in Africa. F_{Tot}, F_{Dry}, F_{Wet} represent the total, dry and wet N deposition, respectively. C_{NH3} and C_{NO2} are the satellite NH_3 and NO_2 concentrations, respectively. E_{NH3} and E_{NOx} are the emissions of NH_3 and NO_x respectively. MAP is the mean annual precipitation. GDPpc is the gross domestic product per capita. R represents the correlation coefficient. The symbols ***, **, *, and – represent significance at $P < 0.0001$, $P < 0.001$, $P < 0.05$, and no significant, respectively. Greyed out boxes indicate no data.

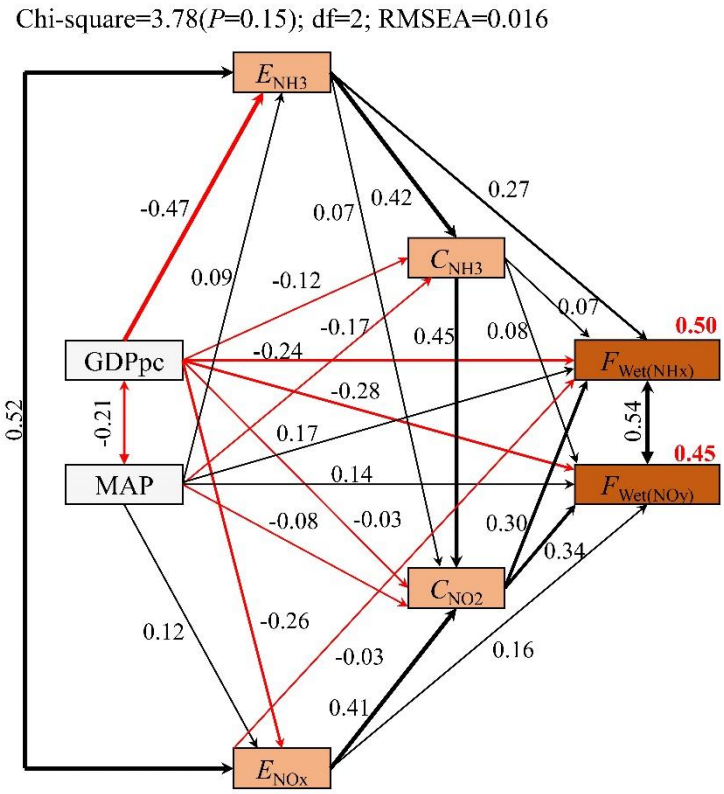

Supplementary Figure 9 | Structural equation model of wet deposition. $F_{Wet(NHx)}$ is wet ammonium deposition, $F_{Wet(NOy)}$ is wet nitrate deposition. C_{NH3} and C_{NO2} are the satellite NH_3 and NO_2 concentrations, respectively. E_{NH3} and E_{NOx} are the emissions of NH_3 and NO_x, respectively. MAP is the mean annual precipitation. GDPpc is the gross domestic product per capita. Red and black arrows represent the negative and positive relationships and numbers on them the correlation or regression coefficients. The greater the coefficients, the thicker the line.

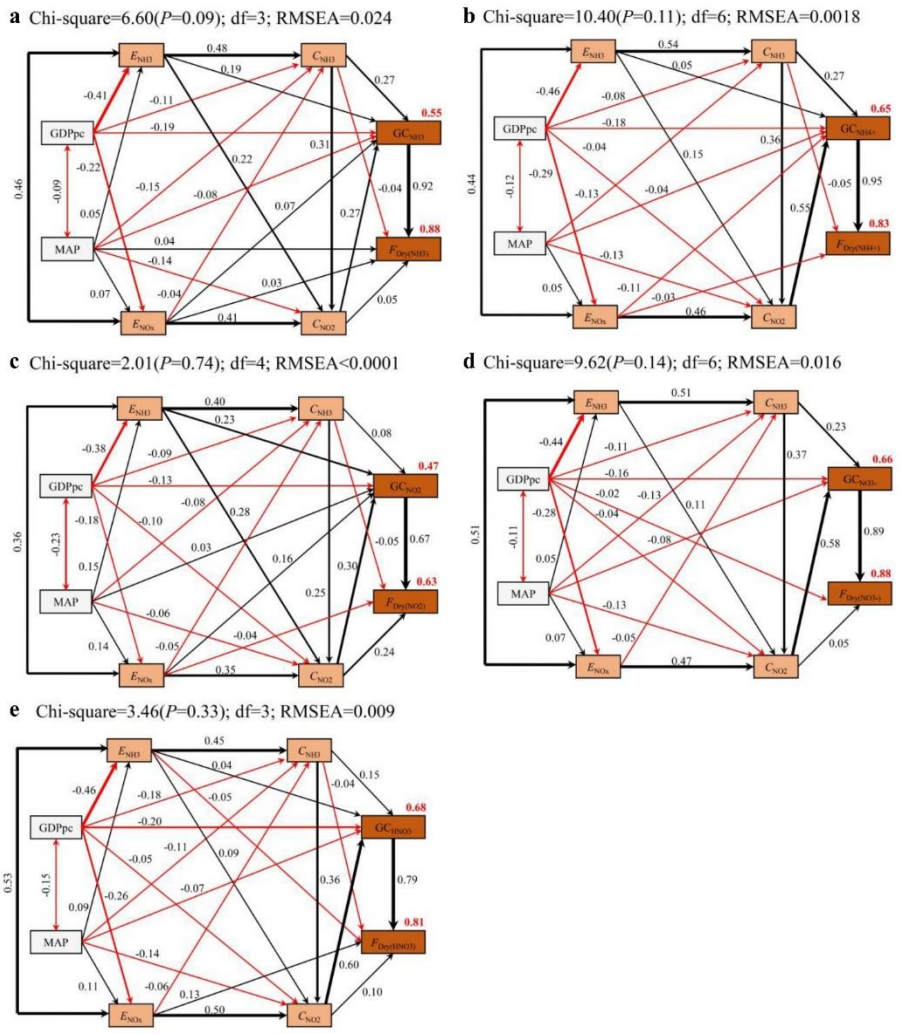

Supplementary Figure 10 | Structural equation models of dry deposition. (a) dry gaseous NH_3 deposition ($F_{Dry(NH3)}$) and ground gaseous NH_3 concentration (GC_{NH3}); (b) dry particulate NH_4^+ deposition ($F_{Dry(NH4+)}$) and ground particulate NH_4^+ concentration (GC_{NH4+}); (c) dry gaseous NO_2 deposition ($F_{Dry(NO2)}$) and ground gaseous NO_2 concentration (GC_{NO2}); (d) dry particulate NO_3^- deposition ($F_{Dry(NO3-)}$) and ground particulate NO_3^- concentration (GC_{NO3-}); (e) dry gaseous HNO_3 deposition ($F_{Dry(HNO3)}$) and ground gaseous HNO_3 concentration (GC_{HNO3}). C_{NH3} and C_{NO2} are the satellite NH_3 and NO_2 concentrations, respectively. E_{NH3} and E_{NOx} are the emissions of NH_3 and NO_x, respectively. MAP is the mean annual precipitation. GDPpc is the gross domestic product per capita. Red and black arrows represent the negative and positive relationships and numbers on them the correlation or regression coefficients. The greater the coefficients, the thicker the line.

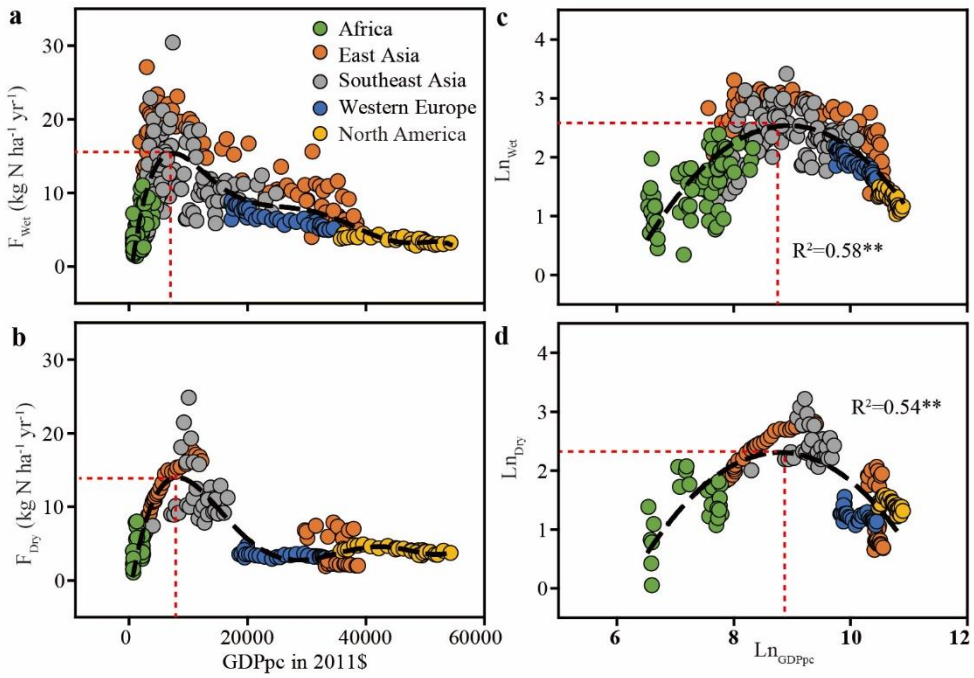

Supplementary Figure 11 | The relationship between wet and dry nitrogen deposition and gross domestic product per capita. (a) Relationship between wet nitrogen deposition and gross domestic product per capita (GDPpc). (b) Relationship between dry nitrogen deposition and GDPpc. (c) Relationship between the natural logarithm transformations of wet nitrogen deposition and GDPpc. (d) Relationship between the natural logarithm transformations of dry nitrogen deposition and GDPpc. F_{Wet} and F_{Dry} represent wet and dry deposition, respectively. Ln_{Wet} and Ln_{Dry} are the natural logarithm transformations of F_{Wet} and F_{Dry} respectively. The data used in a and b are observations of N deposition and GDPpc, and those in c and d the logarithmic values of nitrogen deposition and GDPpc. African countries are Niger, Mali, Cameroon and Cote d'Ivoire. Southeast Asian countries are Vietnam, Malaysia, Indonesia and Thailand. East Asian countries are China, South Korea and Japan. Western European countries are EU countries (the EU27). North American countries are the United States and Canada. R^2 represents the coefficient of determination. ** and * indicate significance levels at $P = 0.01$ and $P = 0.05$, respectively.

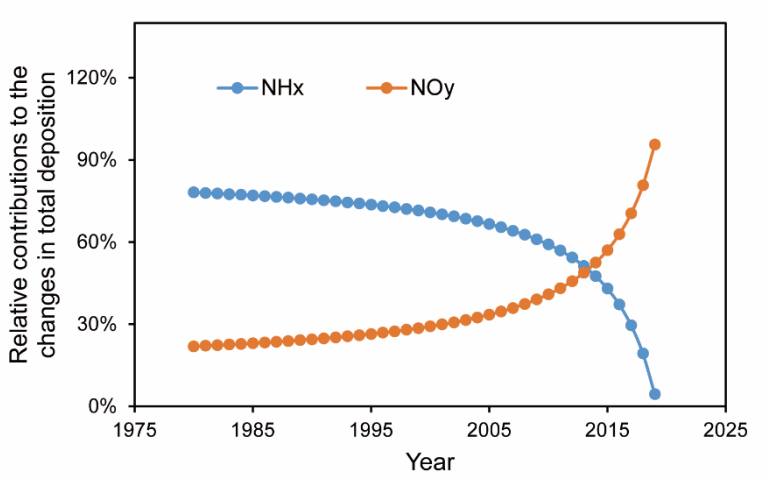

Supplementary Figure 12 | Relative contribution of NHx and NOy deposition to changes in global total nitrogen deposition. Results were calculated using the first derivatives from the fitted equation of global total nitrogen deposition changes between 1980 and 2020.

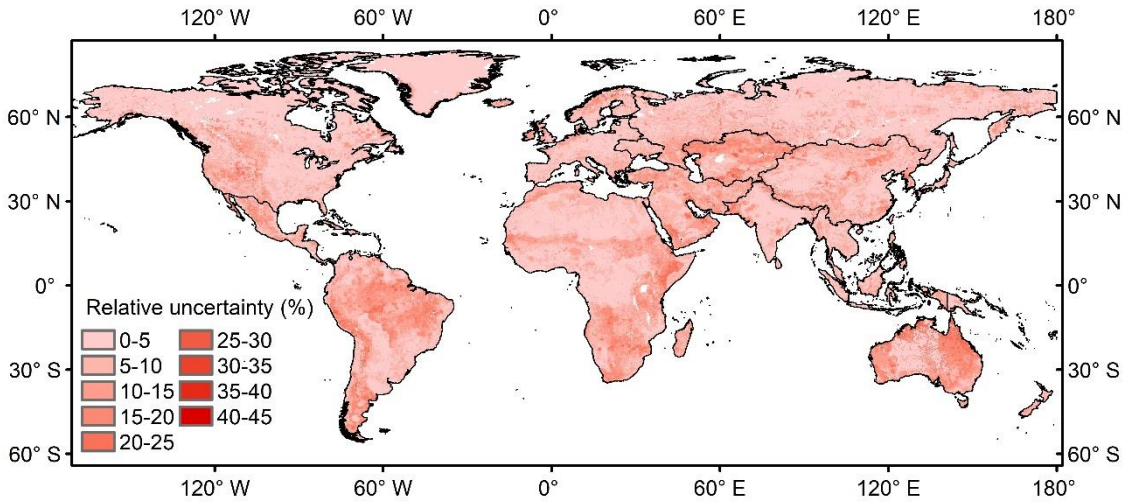

Supplementary Figure 13 | The relative uncertainty of global nitrogen deposition. The relative uncertainty at each pixel were calculated across three models. The relative uncertainty was defined as the ratio of standard error to the mean value of three models. The darker the red color, the greater the value.

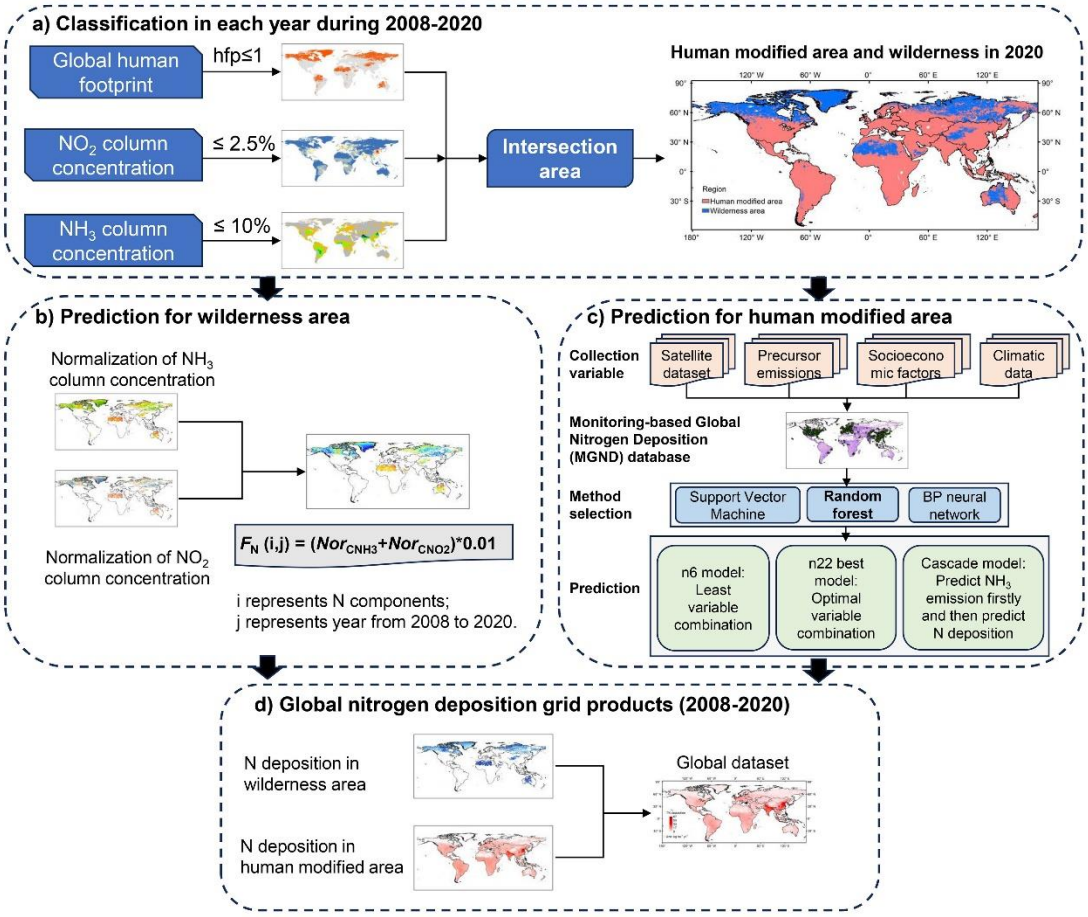

Supplementary Figure 14 | Framework for generating the global nitrogen deposition grid dataset in this study. (a) Classification for each year from 2008 to 2020. Global land is classified into two categories based on global human footprint data, and satellite NH_3 and NO_2 concentrations. (b) Prediction for wilderness areas. These areas are less affected by anthropogenic activities, and nitrogen deposition is estimated using satellite NH_3 and NO_2 concentrations. (c) Prediction for human-modified areas. Machine learning methods are used to upscale nitrogen deposition from site scale to global grid scale in these areas. (d) Global nitrogen deposition grid products (2008–2020). The nitrogen deposition datasets for wilderness and human-modified areas are combined to create a global dataset of nitrogen deposition flux for 2008–2020, with a spatial resolution of 0.125° × 0.125°.

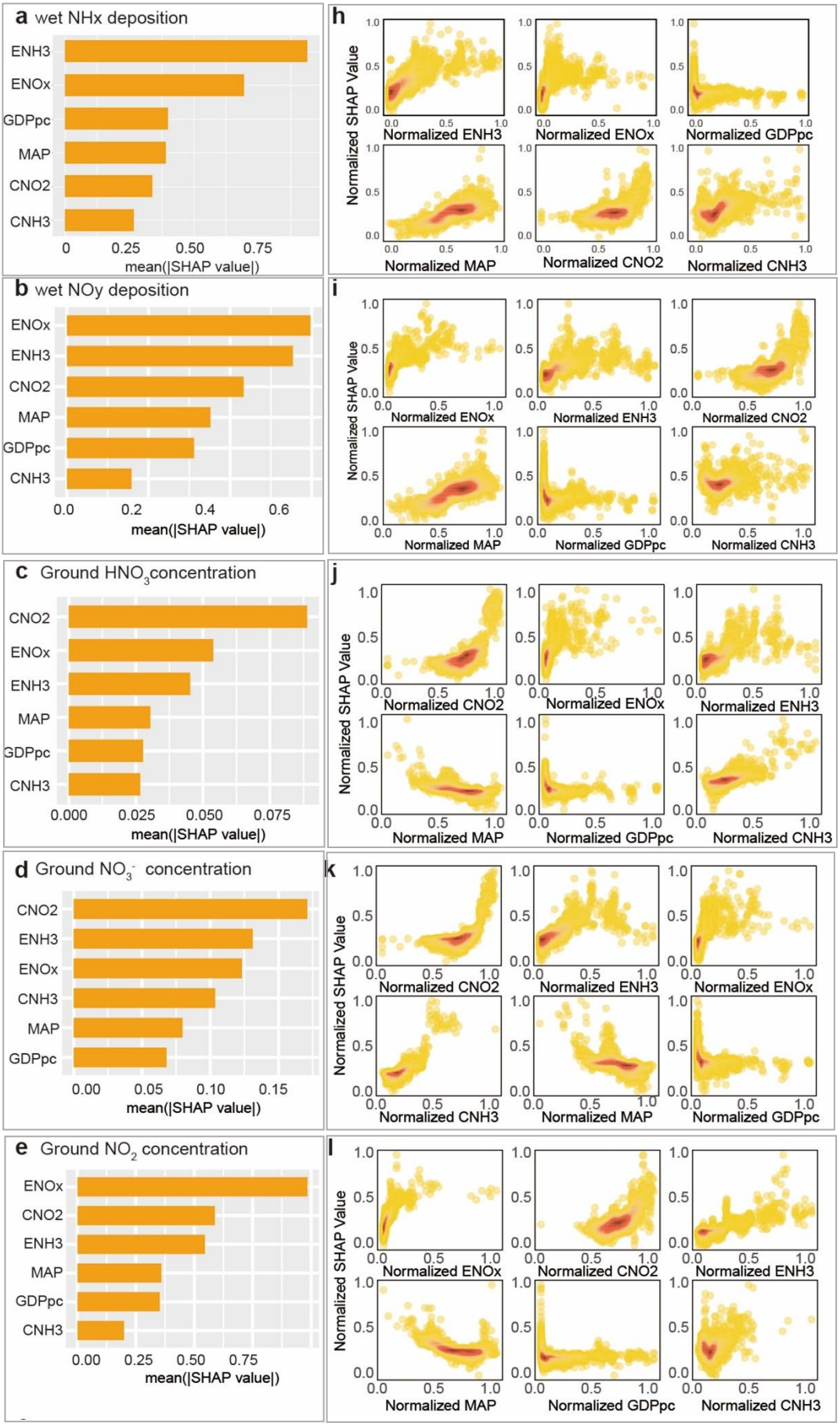
a wet NHx deposition
ENH3
ENOx
GDPpc
MAP
CNO2
CNH3
0
0.25
0.50
0.75
mean(|SHAP value|)
b wet NOy deposition
ENOx
ENH3
CNO2
MAP
GDPpc
CNH3
0.0
0.2
0.4
0.6
mean(|SHAP value|)
c Ground HNO3concentration
CNO2
ENOx
ENH3
MAP
GDPpc
CNH3
0.000
0.025
0.050
0.075
mean(|SHAP value|)
d Ground NO3- concentration
CNO2
ENH3
ENOx
CNH3
MAP
GDPpc
0.00
0.05
0.10
0.15
mean(|SHAP value|)
e Ground NO2 concentration
ENOx
CNO2
ENH3
MAP
GDPpc
CNH3
0.00
0.25
0.50
0.75
mean(|SHAP value|)
h
Normalized SHAP Value
Normalized ENH3
Normalized ENOx
Normalized GDPpc
Normalized MAP
Normalized CNO2
Normalized CNH3
i
Normalized SHAP Value
Normalized ENOx
Normalized ENH3
Normalized CNO2
Normalized MAP
Normalized GDPpc
Normalized CNH3
j
Normalized SHAP Value
Normalized CNO2
Normalized ENOx
Normalized ENH3
Normalized MAP
Normalized GDPpc
Normalized CNH3
k
Normalized SHAP Value
Normalized CNO2
Normalized ENH3
Normalized ENOx
Normalized CNH3
Normalized MAP
Normalized GDPpc
l
Normalized SHAP Value
Normalized ENOx
Normalized CNO2
Normalized ENH3
Normalized MAP
Normalized GDPpc
Normalized CNH3

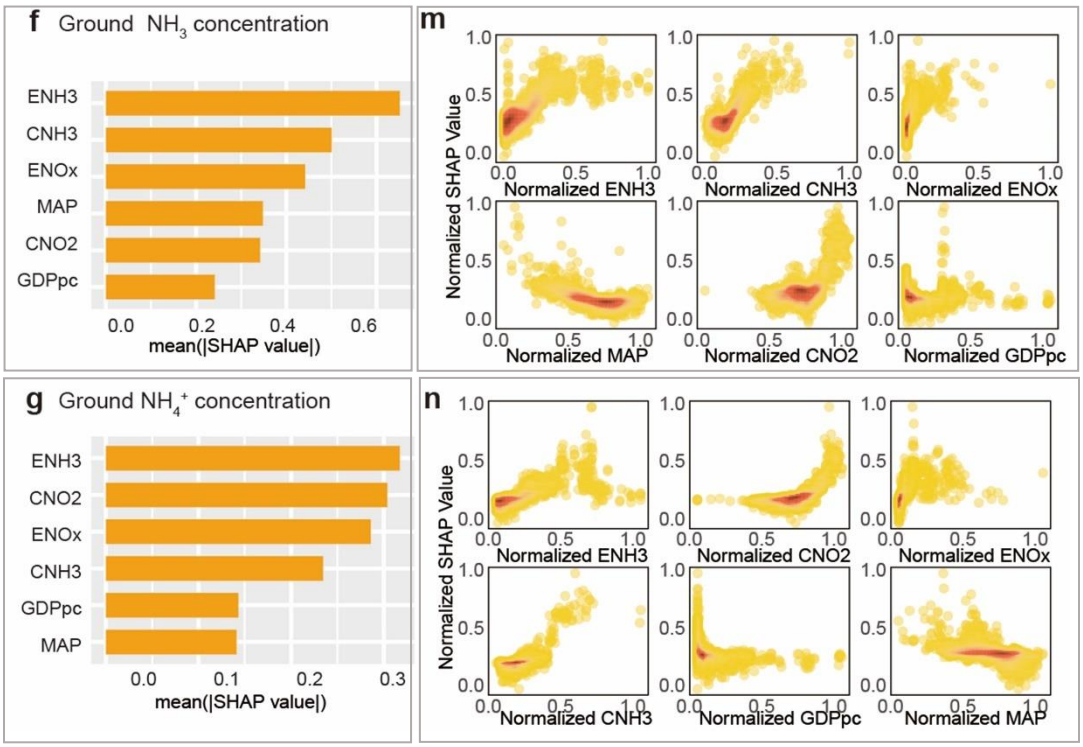

Supplementary Figure 15 | Predictors of the n6 model. (a-g) Importance of each predictor in predicting global nitrogen deposition. (h-n) Responses of Sharply values to the six predictors. The colors in the main plot indicate sample density (high density shown in dark orange). C_{NH_3} and C_{NO_2} represent satellite NH_3 and NO_2 concentrations, respectively. E_{NH_3} and E_{NOx} denote emissions of NH_3 and NOx, respectively. MAP stands for mean annual precipitation, and GDPpc refers to gross domestic product per capita.

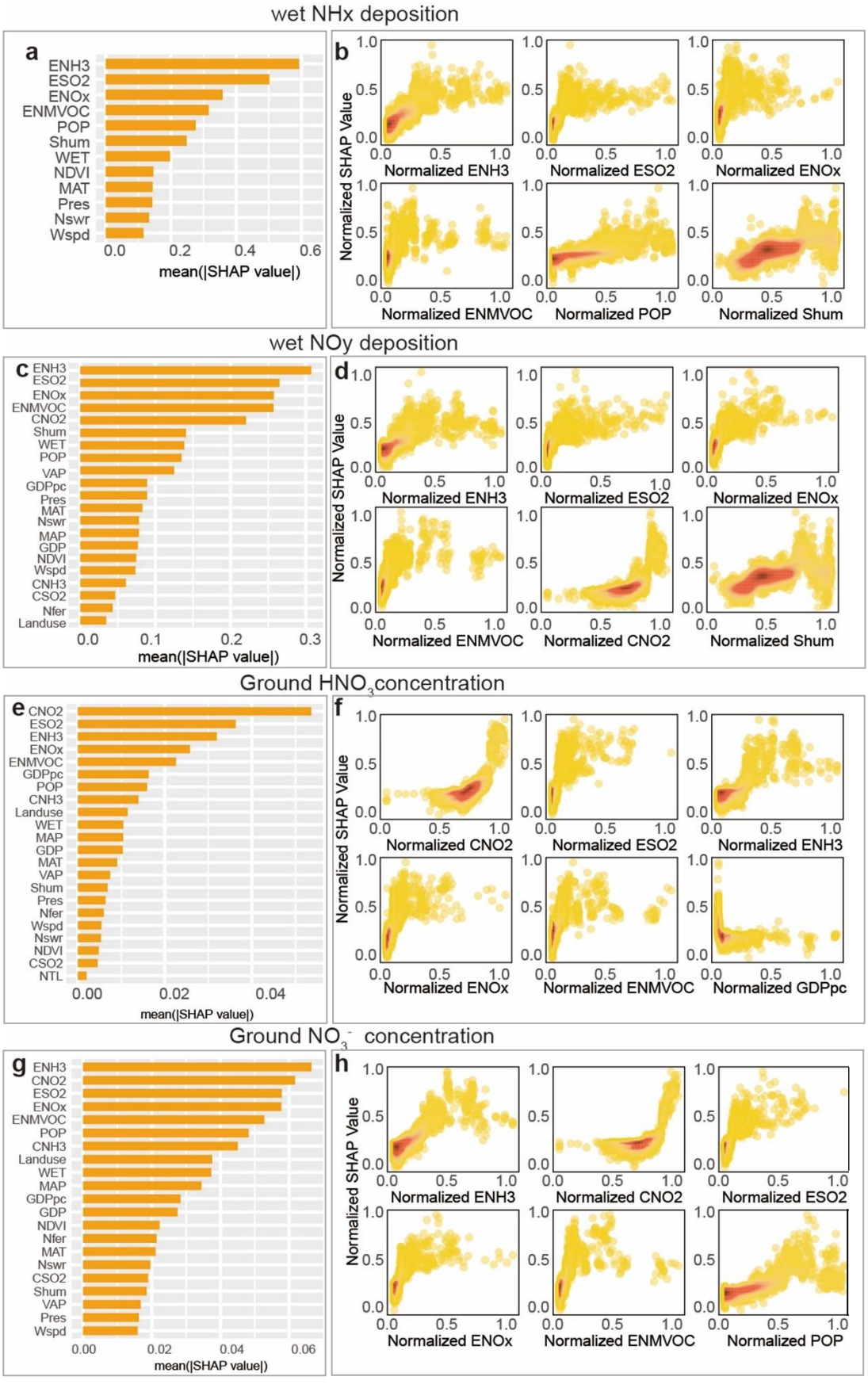
wet NHx deposition
a
ENH3
ESO2
ENOx
ENMVOC
POP
Shum
WET
NDVI
MAT
Pres
Nswr
Wspd
0.0
0.2
0.4
0.6
mean(|SHAP value|)
b
Normalized SHAP Value
Normalized ENH3
Normalized ESO2
Normalized ENOx
Normalized ENMVOC
Normalized POP
Normalized Shum
wet NOy deposition
c
ENH3
ESO2
ENOx
ENMVOC
CNO2
Shum
WET
POP
VAP
GDPpc
Pres
MAT
Nswr
MAP
GDP
NDVI
Wspd
CNH3
CSO2
Nfer
Landuse
0.0
0.1
0.2
0.3
mean(|SHAP value|)
d
Normalized SHAP Value
Normalized ENH3
Normalized ESO2
Normalized ENOx
Normalized ENMVOC
Normalized CNO2
Normalized Shum
Ground HNO3 concentration
e
CNO2
ESO2
ENH3
ENOx
ENMVOC
GDPpc
POP
CNH3
Landuse
WET
MAP
GDP
MAT
VAP
Shum
Pres
Nfer
Wspd
Nswr
NDVI
CSO2
NTL
0.00
0.02
0.04
mean(|SHAP value|)
f
Normalized SHAP Value
Normalized CNO2
Normalized ESO2
Normalized ENH3
Normalized ENOx
Normalized ENMVOC
Normalized GDPpc
Ground NO3- concentration
g
ENH3
CNO2
ESO2
ENOx
ENMVOC
POP
CNH3
Landuse
WET
MAP
GDPpc
GDP
NDVI
Nfer
MAT
Nswr
CSO2
Shum
VAP
Pres
Wspd
0.00
0.02
0.04
0.06
mean(|SHAP value|)
h
Normalized SHAP Value
Normalized ENH3
Normalized CNO2
Normalized ESO2
Normalized ENOx
Normalized ENMVOC
Normalized POP

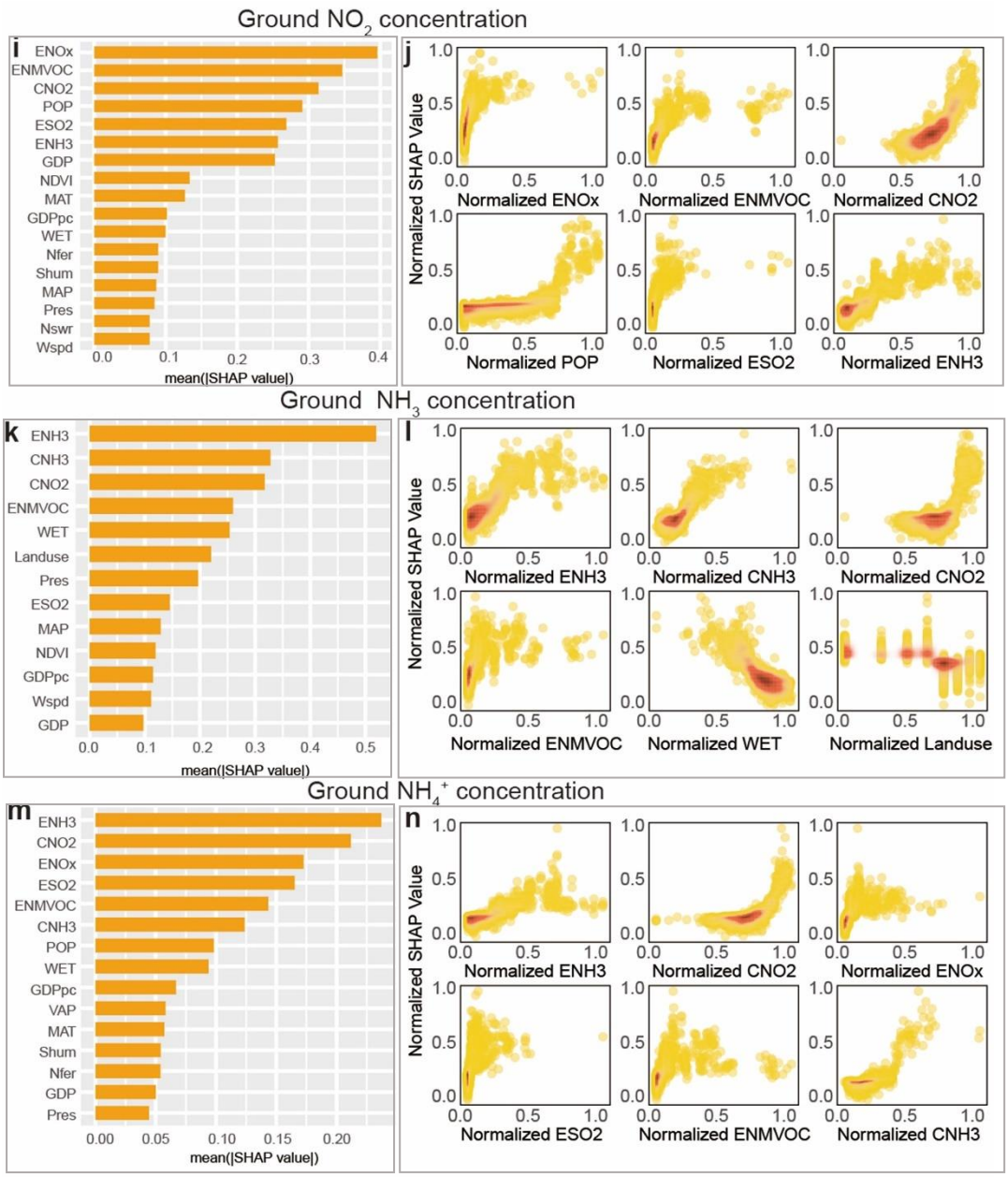

Supplementary Figure 16 | Predictors of n22-best model. (a, c, e, g, i, k, m) Importance of each predictor in predicting global nitrogen deposition. (b, d, f, h, j, l, n) Responses of Sharply values to the top six most important predictors. The colors in the main plot indicate sample density (high density shown in dark orange). CNH_3, CNO_2, and CSO_2 represent satellite NH_3, NO_2, and SO_2 concentrations, respectively. ENH_3, ENOx, ESO_2, and ENMVOC denote emissions of NH_3, NOx, SO_2, and non-methane volatile organic compounds (NMVOC), respectively. MAP is mean annual precipitation, MAT is mean annual temperature, WET indicates the number of wet days, VAP is vapor pressure, Nswrs is net shortwave radiation flux, Pres is surface pressure, Shum is specific humidity, Wspd is wind speed, NDVI is the Normalized Difference Vegetation Index, Landuse refers to land use data from Global Production–Living–Ecological Space data, Nfer represents nitrogen fertilizer use, GDP is gross domestic product, GDPpc is gross domestic product per capita, POP is population, and NTL is night light.

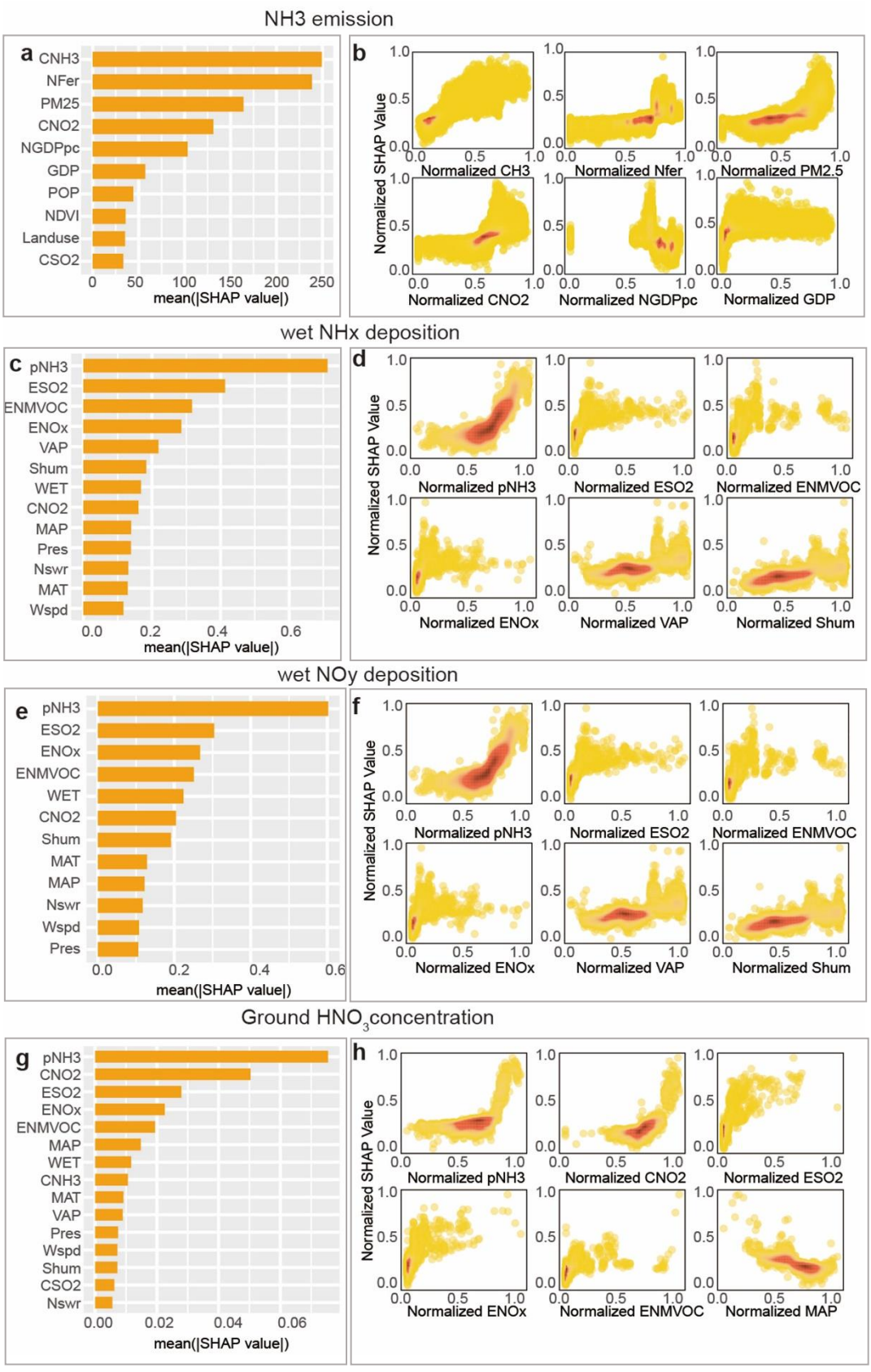
NH3 emission
a
CNH3
NFer
PM25
CNO2
NGDPpc
GDP
POP
NDVI
Landuse
CSO2
0 50 100 150 200 250
mean(|SHAP value|)
b
Normalized SHAP Value
Normalized CH3
Normalized Nfer
Normalized PM2.5
Normalized CNO2
Normalized NGDPpc
Normalized GDP
wet NHx deposition
c
pNH3
ESO2
ENMVOC
ENOx
VAP
Shum
WET
CNO2
MAP
Pres
Nswr
MAT
Wspd
0.0 0.2 0.4 0.6
mean(|SHAP value|)
d
Normalized SHAP Value
Normalized pNH3
Normalized ESO2
Normalized ENMVOC
Normalized ENOx
Normalized VAP
Normalized Shum
wet NOy deposition
e
pNH3
ESO2
ENOx
ENMVOC
WET
CNO2
Shum
MAT
MAP
Nswr
Wspd
Pres
0.0 0.2 0.4 0.6
mean(|SHAP value|)
f
Normalized SHAP Value
Normalized pNH3
Normalized ESO2
Normalized ENMVOC
Normalized ENOx
Normalized VAP
Normalized Shum
Ground HNO3concentration
g
pNH3
CNO2
ESO2
ENOx
ENMVOC
MAP
WET
CNH3
MAT
VAP
Pres
Wspd
Shum
CSO2
Nswr
0.00 0.02 0.04 0.06
mean(|SHAP value|)
h
Normalized SHAP Value
Normalized pNH3
Normalized CNO2
Normalized ESO2
Normalized ENOx
Normalized ENMVOC
Normalized MAP

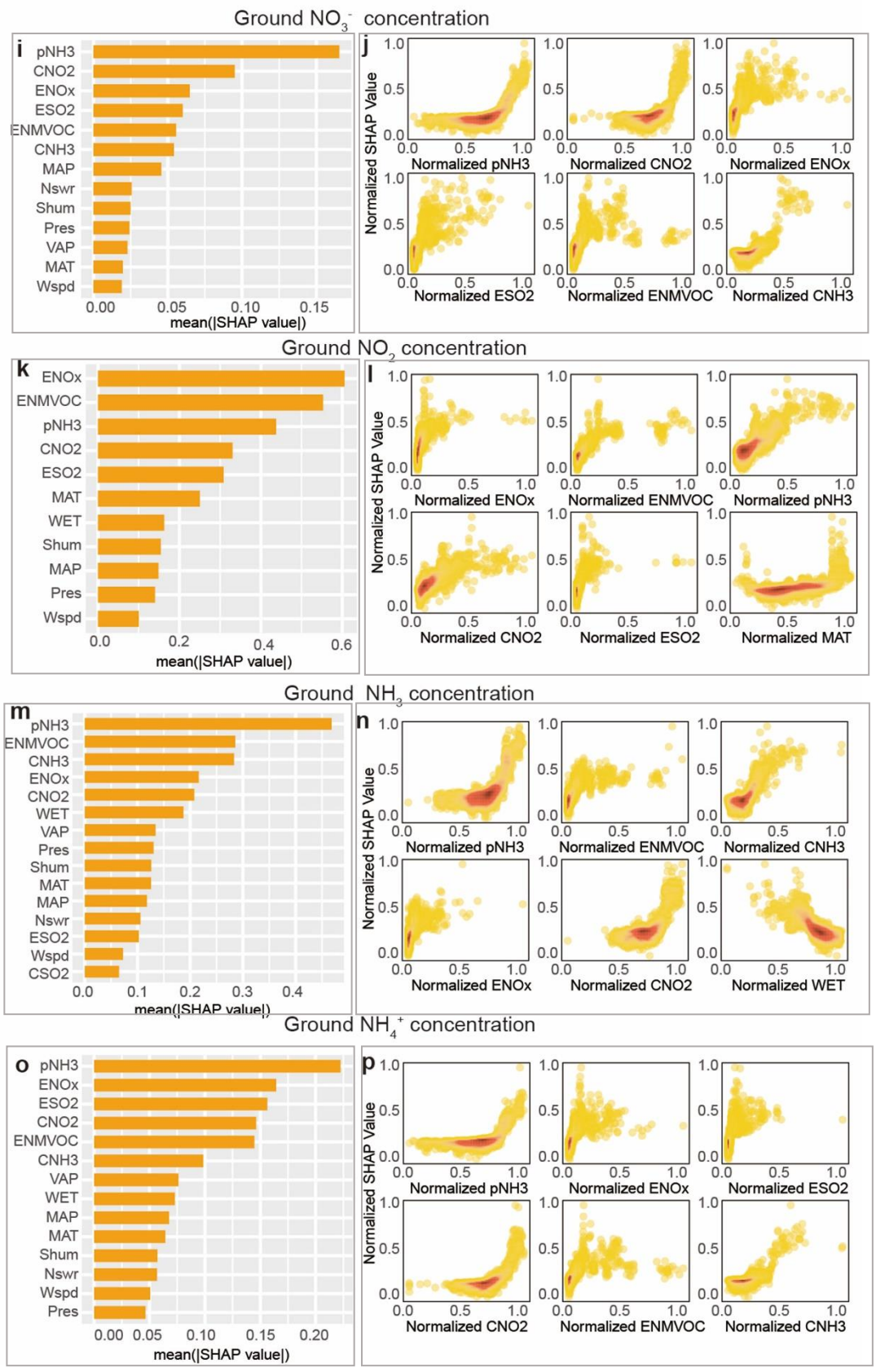

Supplementary Figure 17 | Predictors of cascade model. (a, c, e, g, i, k, m, o) Importance of each predictor in predicting NH_3 emissions and global nitrogen deposition. (b, d, f, h, j, l, n, p) Responses of Sharply values to the

top six most important predictors. The colors in the main plot indicate sample density (high density shown in dark orange). pNH_3 represents the predicted NH_3 emissions. CNH_3, CNO_2, and CSO_2 indicate satellite NH_3, NO_2, and SO_2 concentrations, respectively. ENH_3, ENOx, ESO_2, and ENMVOC denote emissions of NH_3, NOx, SO_2, and non-methane volatile organic compounds (NMVOC), respectively. MAP stands for mean annual precipitation, MAT for mean annual temperature, WET indicates the number of wet days, VAP is vapor pressure, Nswrs is net shortwave radiation flux, Pres is surface pressure, Shum is specific humidity, Wspd is wind speed, NDVI is the Normalized Difference Vegetation Index, Landuse refers to land use data from the Global Production–Living–Ecological Space data, Nfer represents nitrogen fertilizer use, GDP is gross domestic product, GDPpc is gross domestic product per capita, POP is the population, and NTL is night light.

Supplementary Table 1 | Monitoring-based Global Nitrogen Deposition database. $F_{Wet(NHx)}$ represents wet ammonium deposition. $F_{Wet(NOy)}$ represents wet nitrate deposition. $F_{Dry(NH3)}$ represents dry gaseous NH_3 deposition. $F_{Dry(NH4+)}$ represents dry particulate NH_4^+ deposition. $F_{Dry(NO2)}$ represents dry gaseous NO_2 deposition. $F_{Dry(NO3-)}$ represents dry particulate NO_3^- deposition. $F_{Dry(HNO3)}$ represents dry gaseous HNO_3 deposition. $F_{Dry(NHx)}$ represents dry NHx deposition. $F_{Dry(NOy)}$ represents dry NOy deposition. F_{Dry} represents dry nitrogen deposition. F_{Wet} represents wet nitrogen deposition. F_{NHx} represents total NHx deposition. F_{NOy} represents total NOy deposition. F_{Tot} represents total nitrogen deposition.

Variable type	Components	Monitoring site-year		Grid product	
		Year	Site-year	Year	Spatial resolution
Observational variables	$F_{Wet(NHx)}$	1977–2020	12,906	2008–2020	0.125° × 0.125°
	$F_{Wet(NOy)}$	1977–2020	12,902	2008–2020	0.125° × 0.125°
	$F_{Dry(NH3)}$	1986–2021	3,608	2008–2020	0.125° × 0.125°
	$F_{Dry(NH4+)}$	1986–2021	5,156	2008–2020	0.125° × 0.125°
	$F_{Dry(NO2)}$	1980–2020	7,980	2008–2020	0.125° × 0.125°
	$F_{Dry(HNO3)}$	1986–2021	4,872	2008–2020	0.125° × 0.125°
	$F_{Dry(NO3-)}$	1986–2021	5,247	2008–2020	0.125° × 0.125°
	Sum		52,671		
Statistical variables	$F_{Dry(NHx)}$			2008–2020	0.125° × 0.125°
	$F_{Dry(NOy)}$			2008–2020	0.125° × 0.125°
	F_{Dry}			2008–2020	0.125° × 0.125°
	F_{Wet}			2008–2020	0.125° × 0.125°
	F_{NHx}			2008–2020	0.125° × 0.125°
	F_{NHy}			2008–2020	0.125° × 0.125°
	F_{Tot}			2008–2020	0.125° × 0.125°

Supplementary Table 2 | Natural and anthropogenic reactive nitrogen emissions at the global scale. The natural emission data of reactive nitrogen were concluded from Galloway *et al.*[1] and Fowler *et al.*[2]. Community Emission Data System (CEDS)[3], Emissions Database for Global Atmospheric Research (EDGAR)[4], and Luo *et al.*[5]-BUE estimated reactive N emission using a bottom-up approach. Luo *et al.*[5]-TDE and Miyazaki *et al.*[6] estimated reactive N emission using a Top-down approach. Our study estimated NH_3 emission here using random forest model.

Emission（Tg N yr^{-1}）	NOx	NH_3	NHx + NOy
Natural			
Lightening	5-5.4		
Stratosphere	0.6		
Natural soil	18		
Wildfire	0.8	0.8	
Soil and Veg		4.6	
Ocean	5.5	5.6-9	
Subtotal	29.9-30.3	11-14.4	40.9-44.7
Anthropogenic‡			
CEDS [2019]	36.8	50.6	
EDGAR [2018]	37.7	48.0	
Luo et al. (2022)-BUE [2018]		68.9	
Luo et al. (2022)-TDE [2018]		87.3	
Miyazaki et al. (2017) [2014]	47.5		
This study [2020]		57.9	
Subtotal	36.8-47.5	48.0-87.3	84.8-134.8
Total	66.7-77.8	59.0-101.7	125.7-179.5

Supplementary Table 3 | Parameters and evaluation of EKC equations. Note: (i) $\beta_3 = \beta_2 = \beta_1 = 0$. There was no relationship between GDP_{pc} and nitrogen deposition. (ii) $\beta_1 > 0$, $\beta_3 = \beta_2 = 0$. A linear relationship. (iii) $\beta_1 < 0$, $\beta_3 = \beta_2 = 0$. A monotonic decreasing relationship. (iv) $\beta_1 > 0$, $\beta_2 < 0$, $\beta_3 = 0$. A Normal Distribution (inverted U-shaped) relationship, that is, EKC. (v) $\beta_1 < 0$, $\beta_2 > 0$, $\beta_3 = 0$. A U-shaped relationship. (vi) $\beta_1 > 0$, $\beta_2 < 0$, $\beta_3 > 0$. A N-shaped relationship. (vii) $\beta_1 < 0$, $\beta_2 > 0$, $\beta_3 < 0$. Inverted N-shaped Relationship. F_{Dry} represents dry nitrogen deposition. F_{Wet} represents wet nitrogen deposition. F_{NHx} represents total NHx deposition. F_{NOy} represents total NOy deposition. F_{Tot} represents total nitrogen deposition. $ represents U.S. dollar.

Component	α	β_1	β_2	β_3	R^2	*P*	Peak (2011 $)
F_{Tot}	−22.29	5.82	−0.32	0	0.72	0.001	8,899
F_{NHx}	−26.01	6.69	−0.38	0	0.73	0.001	6,652
F_{NOy}	−19.87	4.84	−0.26	0	0.56	0.001	11,022
F_{Wet}	−24.14	5.97	−0.33	0	0.58	0.001	8,480
F_{Dry}	−23.25	5.81	−0.32	0	0.54	0.001	8,762

Supplementary Table 4 | N emission and deposition in North America, Western Europe and China. The Multi-resolution Emission Inventory for China (MEIC)[7] was available at http://www.meicmodel.org. Input4MIPs data was available at https://pcmdi.llnl.gov/search/input4mips/. CCMI data was available at https://blogs.reading.ac.uk/ccmi/.

Regions	Emission（Tg N yr^{-1}）				Deposition（Tg N yr^{-1}）			
	Source	NOx	NH_3	Sum	Source	NOx	NH_3	Sum
North America	CEDS [2019]	2.85	3.39	6.24	Input4MIPs [2014]	4.71	3.38	8.09
	EDGAR [2018]	3.89	4.13	8.02	CCMI [2018]	3.66	3.39	7.05
	Luo et al. (2022)-TDE [2018]		5.38		Ackerman et al., 2019 [2016][8]	3.15	3.55	6.7
					This study [2020]	2.72	4.73	7.45
Western Europe	CEDS [2019]	2.03	3.87	5.9	Input4MIPs (2014)	1.98	2.78	4.77
	EDGAR [2018]	2.52	4.95	7.47	CCMI [2018]	1.65	2.53	4.18
	Luo et al. (2022)-TDE [2018]		5.05		Ackerman et al (2019), [2016]	1.44	2.91	4.35
					This study [2020]	1.75	2.56	4.31
China	CEDS [2019]	6.89	10.11	17	Input4MIPs (2014)	4.31	5.92	10.23
	EDGAR [2018]	7.19	6.82	13.98	CCMI [2018]	5.02	6.40	11.42
	Luo et al. (2022)-TDE [2018]		10.82		Ackerman et al (2019), [2016]	4.79	7.57	12.36
	MEIC (2020)	6.02	7.47	13.49	This study [2020]	5.08	7.20	12.28

Supplementary Table 5 | Data sources and information of variables

Dataset	Variables	Time series	Spatial resolution	Reference
Climatic Research Unit (CRU) cru_ts4.07	Mean annual precipitation (MAP), Mean annual temperature (MAT), Wet days (WET), Vapour pressure (VAP)	1991-2022, monthly	0.5°*0.5°	Harris et al. (2020) [9]
NCEP-NCAR Reanalysis 1	net shortwave radiation flux (Nswrs), surface pressure (Pres), specific humidity (Shum), wind speed (Wspd)	1948-2022, monthly	1.875°*1.915°	Kalnay et al. (1996)[10]. NCEP-NCAR Reanalysis 1 data provided by the NOAA PSL, Boulder, Colorado, USA, from their website at https://psl.noaa.gov
CEDS v_2021_04_21 gridded emissions data	NH_3, NOx, NMVOC, SO_2 emission (E_{NH3}, E_{NOx}, E_{NMVOC}, E_{SO2})	1750-2019, monthly	0.5°*0.5°	O'Rourke et al. (2021)[3]
Standard monthly IASI/Metop-A ULB-LATMOS ammonia (NH3) L3 product (total column)	NH_3 column concentration (C_{NH3})	2008-2020, monthly	1°*1°	Van Damme et al., (2017)[11]
OMI NO_2: QA4ECV version 1.1	NO_2 column concentration (C_{NO2})	2004-2021, monthly	0.125°*0.125°	Boersma et al. (2011)[12]
OMI/Aura Sulfur Dioxide (SO_2) Total Column Daily L3	SO_2 column concentration (C_{SO2})	2004-2023, daily	0.25°*0.25°	Li et al. (2020)[13]
Satellite-derived PM2.5	PM2.5	1998-2021, monthly	0.0045°*0.0045°	van Donkelaar et al. (2021)[14]
Global NPP-VIIRS-Like Nighttime Light Data	Nighttime Light (NTL)	2000–2022, annual	500 m	Chen et al. (2021)[15]
LandScan Global	Population	2000-2022, annual	1 km	Sims et al. (2023)[16]
Global 1 km × 1 km gridded revised real gross domestic product	gross domestic product (GDP)	1992-2019, annual	1 km	Chen et al. (2022)[17]
MOD13C2 - MODIS/Terra Vegetation Indices Monthly L3 Global 0.05Deg CMG	Normalized Difference Vegetation Index (NDVI)	2000-2022, monthly	0.05°*0.05°	Didan et al. (2015)[18]
Global production–living–ecological space data	Land use	2000, 2010, 2020	1 km	Fu et al. (2023)[19]
National Nutrient nitrogen N Use per area of cropland	nitrogen-fertilizer-application-per-hectare-of-cropland (NNfer)	1961-2020	Country	FAO (2021)[20]
GDP per capita, Maddison Project database 2020	gross domestic product per capita (GDPpc)	1990-2021	Country	Bolt and Jan (2020)[21]
Global crop-specific nitrogen fertilization dataset	Crop-specific N application rate (Nfer)	1961-2020	5 arc-min	Adalibieke et al. (2023)[22]
Global terrestrial Human Footprint dataset	Human Footprint (HFP)	2000-2020	1 km	Mu et al. (2022)[23]

Supplementary Table 6 | Comparison of different machine learning methods

Component	Random forest Model					Support Vector Machine				BP neural network			
	Var explained (%)	Training		Testing		Training		Testing		Training		Testing	
		R^2	RMSE	R^2	RMSE	R^2	RMSE	R^2	RMSE	R^2	RMSE	R^2	RMSE
Wet NOy deposition	76.57	0.97	0.56	0.83	1.47	0.62	1.92	0.54	1.93	0.59	0.06	0.53	0.06
Wet NHx deposition	77.34	0.97	0.66	0.75	1.92	0.60	2.20	0.55	2.61	0.60	0.06	0.55	0.06
Ground NH_3 concentration	79.13	0.97	0.52	0.84	1.52	0.62	1.94	0.63	1.72	0.60	0.09	0.59	0.08
Ground NH_4^+ concentration	83.25	0.98	0.36	0.93	0.48	0.74	1.19	0.68	1.15	0.75	0.03	0.67	0.03
Ground NO_3^- concentration	73.78	0.88	0.38	0.82	0.48	0.78	0.53	0.67	0.51	0.84	0.04	0.67	0.05
Ground NO_2 concentration	84.58	0.98	0.55	0.84	1.21	0.63	2.30	0.74	1.60	0.50	0.07	0.65	0.05
Ground HNO_3 concentration	81.90	0.97	0.06	0.89	0.13	0.77	0.18	0.71	0.20	0.78	0.07	0.67	0.08

Supplementary Table 7 | Parameter and performance of random forest models in this study. pNH_3 represents the predicted NH_3 emissions. CNH_3, CNO_2, and CSO_2 indicate satellite NH_3, NO_2, and SO_2 concentrations, respectively. ENH_3, ENOx, ESO_2, and ENMVOC denote emissions of NH_3, NOx, SO_2, and non-methane volatile organic compounds (NMVOC), respectively. MAP stands for mean annual precipitation, MAT for mean annual temperature, WET indicates the number of wet days, VAP is vapor pressure, Nswrs is net shortwave radiation flux, Pres is surface pressure, Shum is specific humidity, Wspd is wind speed, NDVI is the Normalized Difference Vegetation Index, Landuse refers to land use data from the Global Production–Living–Ecological Space data, Nfer represents nitrogen fertilizer use, GDP is gross domestic product, GDPpc is gross domestic product per capita, POP is the population, and NTL is night light.

Model	Variables	Component	Sample	Hyperparameter			Var explained %	Training		Testing	
				mtry	ntree	Nodesize		R^2	RMSE	R^2	RMSE
n6 model	MAP, GDPpc, C_{NO2}, C_{NH3}, E_{NOx}, E_{NH3}	Wet NHx deposition	3300	2	800	1	72.15	0.97	0.74	0.70	1.89
		Wet NOy deposition	3300	2	800	3	73.70	0.96	0.64	0.67	1.96
		Ground HNO_3 concentration	2141	2	800	1	82.72	0.98	0.06	0.83	0.15
		Ground NO_3^- concentration	2344	1	400	7	75.93	0.92	0.32	0.80	0.38
		Ground NO_2 concentration	2360	2	500	1	81.94	0.98	0.59	0.79	1.55
		Ground NH_4^+ concentration	2906	1	700	1	80.26	0.97	0.40	0.83	0.74
		Ground NH_3 concentration	2081	2	500	2	76.33	0.97	0.57	0.82	1.47
n22 best model	E_{NH3}, E_{NOx}, E_{NMVOC}, E_{SO2}, C_{NH3}, C_{NO2}, C_{SO2}, MAP, MAT, WET, VAP, Nswrs, Pres, Shum, Wspd, NTL, GDP, POP, GDPpc, Nfer, NDVI, land use	Wet NHx deposition	3300	2	700	1	77.34	0.97	0.66	0.75	1.92
		Wet NOy deposition	3300	3	800	1	76.57	0.97	0.56	0.83	1.47
		Ground HNO_3 concentration	2124	4	700	3	81.90	0.97	0.06	0.89	0.13
		Ground NO_3^- concentration	2218	1	600	15	73.78	0.88	0.38	0.82	0.48
		Ground NO_2 concentration	2228	2	800	1	84.58	0.98	0.55	0.84	1.21
		Ground NH_4^+ concentration	2741	2	500	1	83.25	0.98	0.36	0.93	0.48
		Ground NH_3 concentration	2034	3	900	1	79.13	0.97	0.52	0.84	1.50
Cascade model	C_{NH3}, C_{NO2}, C_{SO2}, NTL, GDP, POP, GDPpc, Nfer, NDVI, landuse	Predict NH_3 emission	124110	5	1000	1	98.04	0.99	75.77	0.98	171.4
	pNH_3, C_{NH3}, C_{NO2}, C_{SO2}, E_{NOx}, E_{NMVOC}, E_{SO2}, MAP, MAT, WET, VAP, Nswrs, Pres, Shum, Wspd	Wet NHx deposition	3558	2	900	1	75.14	0.97	0.66	0.75	1.79
		Wet NOy deposition	3558	2	700	1	75.45	0.97	0.57	0.74	1.48
		Ground HNO_3 concentration	2306	4	600	3	82.55	0.97	0.06	0.88	0.11
		Ground NO_3^- concentration	2430	2	900	13	76.80	0.91	0.31	0.79	0.49
		Ground NO_2 concentration	2440	3	700	1	82.86	0.98	0.57	0.88	1.16
		Ground NH_4^+ concentration	2938	1	1000	1	83.71	0.98	0.34	0.82	0.79
		Ground NH_3 concentration	2209	2	700	1	75.40	0.97	0.55	0.83	1.24

Supplementary Table 8 | Regional N deposition flux and total input in 2020 from 3 models

Regions	Cascade model				n24 best model				n6 model			
	F_N (kg ha^{-1} yr^{-1})			N input (Tg N yr^{-1})	F_N (kg ha^{-1} yr^{-1})			N input (Tg N yr^{-1})	F_N (kg ha^{-1} yr^{-1})			N input (Tg N yr^{-1})
	NHx	NOy	Total		NHx	NOy	Total		NHx	NOy	Total	
Africa	4.98	2.45	7.43	22.14	4.41	2.96	7.36	21.94	3.95	2.43	6.37	18.99
Central America	6.22	3.63	9.85	2.59	5.89	4.18	10.07	2.65	4.85	3.37	8.22	2.16
Central Asia	3.09	2.03	5.12	2.05	2.81	1.96	4.77	1.91	1.87	1.56	3.43	1.37
East Asia	6.76	4.91	11.66	13.43	6.82	4.85	11.67	13.44	6.67	4.71	11.38	13.11
East Europe	1.28	1.03	2.30	4.01	1.38	1.05	2.44	4.24	1.34	0.85	2.19	3.81
Greeland	0.14	0.08	0.22	0.05	0.21	0.11	0.32	0.07	0.26	0.11	0.37	0.08
North America	2.50	1.40	3.90	7.37	2.52	1.50	4.02	7.61	2.47	1.43	3.90	7.38
Oceania	3.59	1.50	5.09	4.25	2.48	1.73	4.20	3.50	1.93	1.04	2.97	2.48
South America	6.78	3.83	10.61	18.68	5.38	3.70	9.07	15.97	5.30	2.78	8.08	14.22
South Asia	13.64	9.22	22.86	9.82	13.76	7.68	21.44	9.21	13.32	8.05	21.37	9.18
Southeast Asia	7.59	4.87	12.46	5.33	7.03	5.15	12.18	5.21	6.99	4.74	11.73	5.02
West Asia	3.24	3.03	6.27	4.22	3.18	3.30	6.48	4.36	2.37	2.56	4.93	3.32
West Europe	4.66	3.31	7.97	4.08	5.01	3.47	8.48	4.34	5.29	3.49	8.78	4.50
Global	4.61	2.79	7.40	98.01	4.23	2.90	7.13	94.44	3.96	2.50	6.47	85.60

Supplementary Reference

1. Galloway JN, *et al.* Nitrogen cycles: Past, present, and future. *Biogeochemistry* **70**, 153-226 (2004).
2. Fowler D, *et al.* The global nitrogen cycle in the twenty-first century. *Philos. Trans. R. Soc. B* **368**, 20130164 (2013).
3. O'Rourke PR, *et al.* CEDS v-2021_04_21 Gridded Emissions Data (accessed on 1 Dec 2021, available at https://data.pnnl.gov/dataset/CEDS-4-21-21). (2021).
4. Johansson L, Jalkanen J-P, Kukkonen J. Global assessment of shipping emissions in 2015 on a high spatial and temporal resolution. *Atmos. Environ.* **167**, 403-415 (2017).
5. Luo Z, *et al.* Estimating global ammonia (NH3) emissions based on IASI observations from 2008 to 2018. *Atmos. Chem. Phys.* **22**, 10375-10388 (2022).
6. Miyazaki K, *et al.* Decadal changes in global surface NOx emissions from multi-constituent satellite data assimilation. *Atmos. Chem. Phys.* **17**, 807-837 (2017).
7. Zheng B, *et al.* Trends in China's anthropogenic emissions since 2010 as the consequence of clean air actions. *Atmos. Chem. Phys.* **18**, 14095-14111 (2018).
8. Ackerman D, Millet DB, Chen X. Global estimates of inorganic nitrogen deposition across four decades. *Global Biogeochem. Cycles* **33**, 100-107 (2019).
9. Harris I, Osborn TJ, Jones P, Lister D. Version 4 of the CRU TS monthly high-resolution gridded multivariate climate dataset. *Sci. Data* **7**, 109 (2020).
10. Kalnay E, *et al.* The NCEP/NCAR 40-Year reanalysis project *Journal Bulletin of the American Meteorological Society* **77**, 437-472 (1996).
11. Van Damme M, *et al.* Version 2 of the IASI NH3 neural network retrieval algorithm: near-real-time and reanalysed datasets. *Atmos. Meas. Tech.* **10**, 4905-4914 (2017).
12. Boersma KF, *et al.* An improved tropospheric NO2 column retrieval algorithm for the Ozone Monitoring Instrument. *Atmos. Meas. Tech.* **4**, 1905-1928 (2011).
13. Li C, *et al.* Version 2 Ozone Monitoring Instrument SO2 product (OMSO2 V2): new anthropogenic SO2 vertical column density dataset. *Atmos. Meas. Tech.* **13**, 6175-6191 (2020).
14. van Donkelaar A, *et al.* Monthly global estimates of fine particulate matter and their uncertainty. *Environ. Sci. Technol.* **55**, 15287-15300 (2021).
15. Chen Z, *et al.* An extended time series (2000–2018) of global NPP-VIIRS-like nighttime light data from a cross-sensor calibration. *Earth Syst. Sci. Data* **13**, 889-906 (2021).
16. K. Sims, et al. LandScan Global 2022 (access on 3 Agu 2022, available at https://doi.org/10.48690/1529167). (2022).
17. Chen J, *et al.* Global 1 km × 1 km gridded revised real gross domestic product and electricity consumption during 1992–2019 based on calibrated nighttime light data. *Sci. Data* **9**, 202 (2022).
18. K. Didan, A. Huete, DAAC NL. MOD13C2 MODIS/Terra Vegetation Indices Monthly L3 Global 0.05Deg CMG (access on 5 Jun 2022, available at http://doi.org/10.5067/MODIS/MOD13C2.006). (2015).
19. Fu J, Gao Q, Jiang D, Li X, Lin G. Spatial–temporal distribution of global production–living–ecological space during the period 2000–2020. *Sci. Data* **10**, 589 (2023).
20. FAO. FAOSTAT Fertilizers by Nutrient Database (accessed on 1 Jan 2022, available at https://www.fao.org/faostat/en/#data). (2021).
21. Bolt J, Jan LvZ. Maddison Project Database (accessed on 1 Feb 2022, available at https://www.rug.nl/ggdc/historicaldevelopment/maddison/releases/maddison-project-database-2020). (2020).
22. Adalibieke W, Cui X, Cai H, You L, Zhou F. Global crop-specific nitrogen fertilization dataset in 1961–2020.

Sci. Data **10**, 617 (2023).

23. Mu H*, et al.* A global record of annual terrestrial Human Footprint dataset from 2000 to 2018. *Sci. Data* **9**, 176 (2022).